Continuous Cooling and Isothermal Crystallization of Polycaprolactone

PETER SKOGLUND and ÅKE FRANSSON*

Department of Applied Physics and Electronics, Umeå University, Sweden

SYNOPSIS

In this article we present overall crystallization characteristics of five polycaprolactone samples with mean molecular weights ranging from 50,000 to 400,000. The crystallization temperatures and heats of crystallization are determined as a function of mean molecular weight as well as for cooling rates in the range 0.31 to 40 K/min. Our results show a decrease in crystallization temperature from 320 to 300 K at increasing molecular weight and cooling rate. The heat of crystallization shows a slight decrease within the cooling rate interval and a decrease from about 68 to 48 J/g with increasing molecular weight. We analyze the continuous cooling data according to the Ozawa model for nonisothermal crystallization and compare them with our isothermal data analyzed with the Avrami model. Both the Ozawa and Avrami models give exponent parameters in the range 2.9 to 3.6. In the investigated temperature range and for all samples, we find a nucleation controlled crystallization. At the lowest temperatures, the Ozawa analysis indicates an increasing dependency on limitations in chain mobility. The higher molecular species have in general a slower crystallization rate, with half crystallization times increasing with a factor of about five within the molecular weight range at 320 K.

INTRODUCTION

Polycaprolactone (PCL), with structure —[$(CH_2)_5$-COO]—, belongs to the aliphatic polyesters and is one of the polymers that are known to be biocompatible.[1-7] PCL and its blends have been suggested for use in a wide range of applications. For medical purposes, it may be used in release systems for drug delivery to the human body,[1,2] as a material for surgical devices,[3] or in orthopedics for confection of splints.[4] Outside the medical field, PCL-based products can be used as soil degraded container material or as water-resistant laminate on paper.[5] An interesting application of polymers is as latent heat storages. Polyethylene has been used for this purpose with promising results.[8-13] Polyethyleneoxide and polyethylene glycols with lower melting points have been investigated in low-temperature heat systems.[14,15] In this area, the aliphatic polyesters are interesting because of the possibility to change the crystallization characteristics by altering the number of ethylene units between the ester groups. At high ethylene numbers, their properties will, in principle, approach polyethylene. Material characteristics such as the latent heat, drug permeability, and biodegradability all depend on the crystallinity[1] and, thus, on the crystallization procedure. In general, properties reported are normally based on isothermal crystallization procedures, but common industrial processes usually occur at nonisothermal conditions. In this article we make a comparative study of the overall crystallization behavior of PCL samples of different molecular characteristics at both isothermal and continuous cooling conditions.

EXPERIMENTAL

Methods

The experiments were carried out with a Perkin-Elmer Differential Scanning Calorimeter (DSC-2) equipped with the intracooler II cooling system, and with nitrogen as a purge gas. The low temperature

* To whom correspondence should be addressed.

Journal of Applied Polymer Science, Vol. 61, 2455–2465 (1996)
 CCC 0021-8995/96/132455-11

experiments were performed with liquid nitrogen as a coolant and neon as purge gas. The DSC was calibrated with primary metal standards and alkanes that have thermal properties similar to polymers. Separate calibrations were made for all heating rates. Specific and careful precautions were taken for accurate temperature calibration on cooling. The procedure for this has been reported elsewhere.[16] Crystallization and melting temperatures are defined as the intersection point of the extrapolated baseline and the line of the leading edge of the crystallization/melting curve. Glass transition temperatures are taken as the temperature at which the heat capacity is midway between the liquid and glassy state. Heats of crystallization and melting were deduced according to procedures described by Richardson.[17] Different methods for the peak baseline determination of semicrystalline polymers are also discussed by Alsleben et al.[18,19] Before any crystallization experiment were carried out, the samples were kept at 370 K for 5 min to erase differences in thermal history. In the microscopy studies, we used a Nikon microscope with crossed polarizers.

Material

Two commercial samples, one from Aldrich Chemie (A), one from Union Carbide (B), and three samples (C, D, and E), generously supplied by Dr. P. van de Witte at the University of Twente, Enschede, Netherlands, have been investigated.

All samples were analyzed with Gel Permeation Chromatography (GPC). In Table I, we show the molecular characteristics. All samples were sealed in standard aluminium pans, having masses close to 5 mg, and no changes in mass were detected after the experiments.

RESULTS AND DISCUSSION

In the homogeneous melt at 350 K, all the samples have a specific heat capacity (c_p) of about 1.91 J/g K, in good agreement with the adiabatic value 1.94 J/g K measured by Lebedev and Yevstropov.[20] The calculated value 2.0 J/g K by Wunderlich et al.[21] is somewhat higher. In the rigid state below the glass transition at 160 K, our experimental value of 0.85 J/g K is slightly lower but in satisfactory agreement with those reported by Lebedev and Wunderlich, 0.86 and 0.88 J/g K, respectively. We find glass transition temperatures of $T_g \approx 208$ K and melting temperatures (T_m) close to 325 K, giving a T_g to T_m ratio of 0.64. Ratios close to 2/3 are normally found for linear semicrystalline polymers. Equilibrium melting temperatures compiled by de Juana and Cortazar[22] vary between 329 and 347 K. The T_g values given by the Lebedev,[20] and Wunderlich[21] groups are 209 K for totally amorphous samples, while other literature data[22] are in the range 213–215 K. A glass transition is not a first-order transition and, thus, shows history dependency. The T_g value given above was obtained at a heating rate of 10 K/min after cooling from 380 K to 150 K by 40 K/min and a subsequent 10-min annealing at 150 K. The steps in the specific heat capacity at the glass transition are for all samples close to 0.1 J/g K, indicating no molecular weight dependency. We find that the heat of fusion (Δh_m) after the above-described treatment varies from 70 J/g for sample A of the lowest molecular weight to 57 J/g for sample E of the highest weight. Samples B, C, and D have heats of fusion of 65, 64, and 62 J/g, respectively. All samples show premelting, which starts close to 285 K for sample E, which reveals the broadest melting interval. In Figure 1 we show representative specific heat capacity curves, where the premelting effect and associated increase in the half-width of the melting peaks are readily seen. The melting temperatures vary from 324 to 327 K at a heating rate of 10 K/min, while the peak temperatures remain within 1 K. Literature values of the heat of fusion for 100% crystalline material (Δh_m^0) differ a lot. Crescenzi and co-workers[23] ob-

Table I Molecular Characteristics from GPC Analysis

	Molecular Weight Averages			
Sample	Number Average M_n	Weight Average M_w	Z Average M_z	M_w/M_n
A	22100	55700	90600	2.52
B	40600	92600	165000	2.28
C	51300	147000	342000	2.87
D	78000	217000	536000	2.78
E	116000	378000	956000	3.26

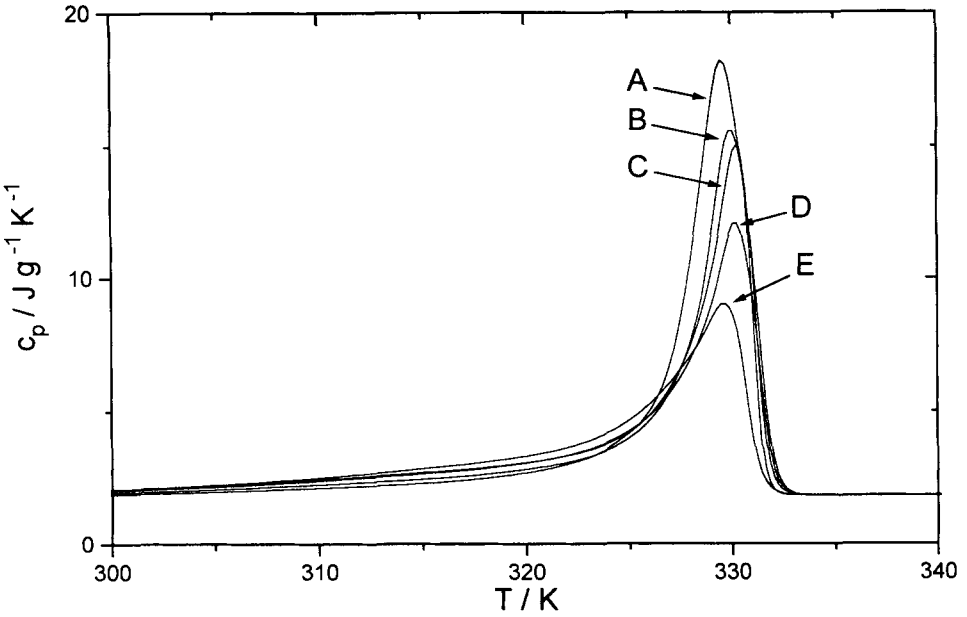

Figure 1 Specific heat capacity vs. temperature. Measured at a heating rate of 10 K/min.

tained 135.4 J/g and 151.9 J/g from melting temperature data for different PCL-diluent mixtures, while their combined study of melting enthalpy and density yielded 139.5 J/g. Lebedev and Yevstropov[20] found a higher value 166.5 J/g, while Wunderlich[21] gives 156.8 J/g. Extrapolating our liquid and glassy c_p values to the glass transition temperature, we get a difference in c_p of 0.6 J/g K, while literature data[20,21] give 0.53 and 0.59 J/g K, respectively. From the extrapolated c_p values at T_g and the observed step in c_p of 0.1 J/g K, we find that the change corresponds to a mobile amorphous degree close to 20% in this semicrystalline polymer. Using Crescenzi's value of 139.5 J/g for Δh_m^0, we calculate a crystalline fraction of 40–50% for our samples and, thus, a rigid amorphous fraction of the order 40–30%. These rigid amorphous chains are trapped by the crystalline parts and will not contribute to the heat capacity in the same sense as the mobile amorphous parts do.

Using 139.5 J/g as the heat of fusion for a 100% crystalline material, Pitt[1] presented the crystallinity as a function of molecular weight in the region 5000 to 50,000 g/mol. At a molecular weight of 50,000 g/mol, he found a crystallinity close to 50% in agreement with our result for sample A. For the other samples, we get crystallinity contents varying from 47 to 41%, decreasing with increasing molecular mass. In Figure 2, we present our crystallinity data together with Pitts. The crystallinity shows an exponential decaying curve with increasing molecular weights, leveling out at a crystallinity close to 40%.

The crystallization temperature (T_c) decreases in general with increasing cooling rate and molecular weight, as can be seen in Figure 3. As discussed later, the crystallization process fulfills mainly at temperatures above the temperature for maximum crystallization rate and is, thus, controlled by nucleation. At the lower cooling rates, there is sufficient time to activate the nucleus, thus giving higher crystallization temperatures. The decrease of T_c with increasing molecular weight is explained by a larger thermodynamic driving force (i.e., larger supercooling) needed for the high molecular samples. However, sample C deviates from the regularity, showing the highest T_c of all samples at the higher cooling rates. This is also seen in Figure 4, where we show the progress of the continuous cooling crystallization. A similar trend of fast crystallization for sample C is observed in the isothermal experiments conducted at 320 and 316 K, and discussed below. We interpret these results as being due to heterogenities with better nucleating abilities compared to the samples A and B. Adding 2% of polyethylene, which have been tested as a substrate for PCL crystallization,[24] to sample A we increased the crystallization temperature by about 5 and 2.5 K at the cooling rates 10 and 1.25 K/min. The increase in T_c by seeding corresponds to a decrease of the time spent in the supercooled melt of 30 and 120 s, respectively, at the given cooling rates. The effect of the added heterogenities on the time needed for the development of a nucleus able to grow, is more pronounced at the lower cooling rates. The difference

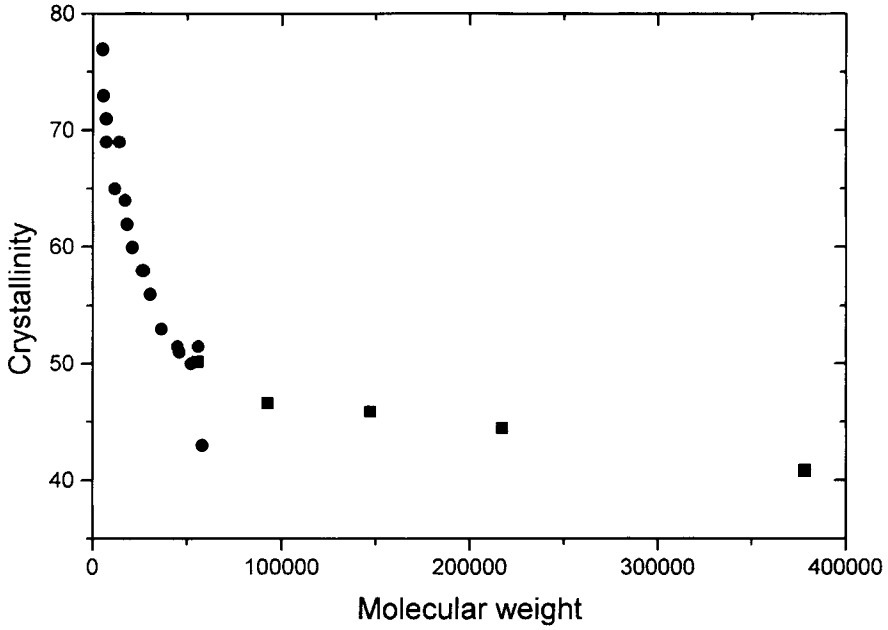

Figure 2 Crystallinity vs. molecular weight, calculated by using 139.5 J/g as the heat of fusion for a 100% crystalline material. Circles, data from Pitt[1]. Squares, data from this work.

in T_c among the samples is 3 K corresponding to about 600 s at the lowest cooling rate (0.31 K/min) and 6 K or 9 s at 40 K/min, with the lowest T_c values found for the high molecular weight sample E. From Figure 4 it is obvious that the crystallization temperature interval increases at higher cooling rates, although the crystallization time decreases with cooling rate. Sample C shows the fastest and most narrow transformation. The absolute value of the resulting heat of crystallization at continuous cooling (Δh_{cc}) is shown in Figure 5, where a slight decrease with increasing cooling rate is observed. The change in Δh_{cc} with cooling rate is of the order 5% for all samples. As the cooling rate increases,

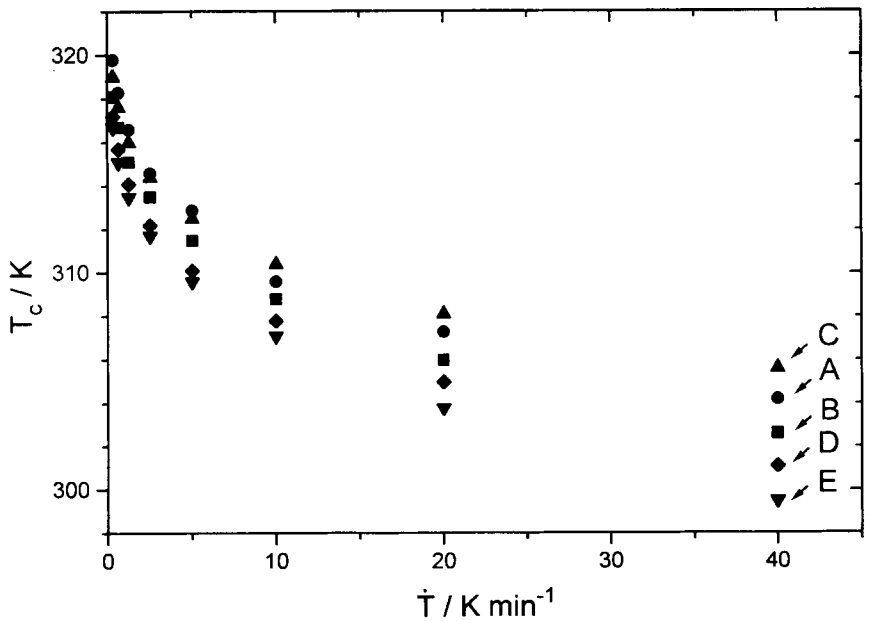

Figure 3 Crystallization temperature vs. cooling rate for samples A, B, C, D, and E.

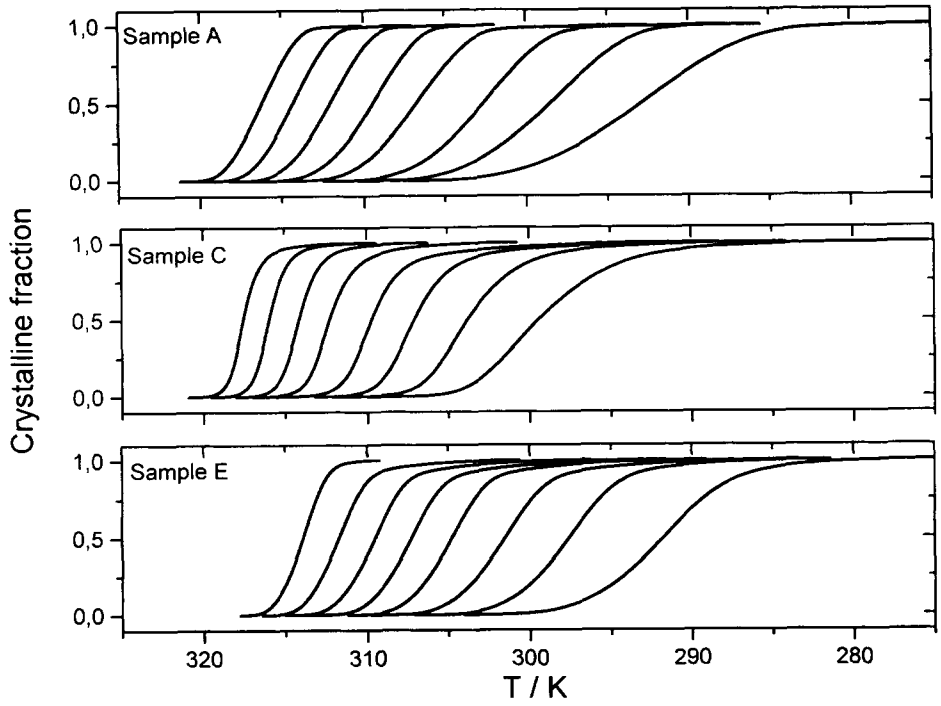

Figure 4 Crystalline fraction as a function of cooling rate and temperature for samples A, C, and E. The cooling rate increases from 0.31 at the left to 40 K/min, doubled in each step.

the crystallization occurs at continuously lower temperatures. At the lowest temperatures, the decreasing mobility of the molecules restrains the crystallization. The sequence of falling Δh_{cc} with increasing molecular weight is explained by the lower mobility of high-molecular weight molecules, giving a lower degree of crystallization and, for that reason, a lower released heat at the crystallization. The dif-

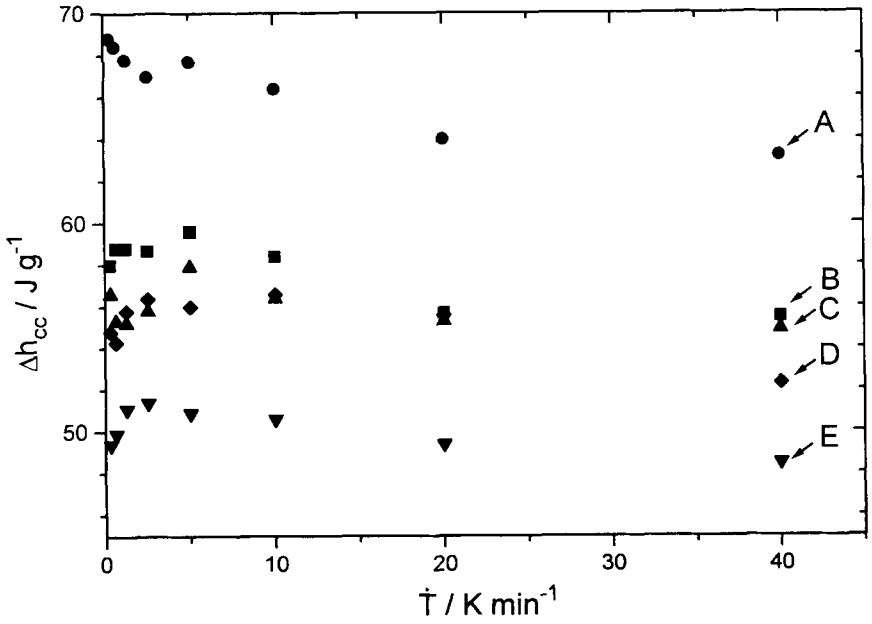

Figure 5 Continuous crystallization energy versus cooling rate for samples A, B, C, D, and E.

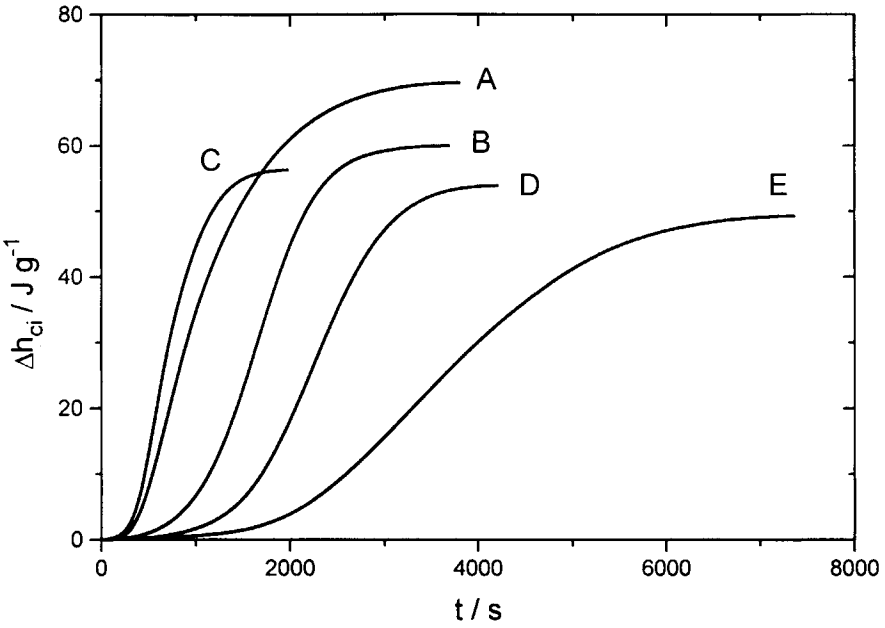

Figure 6 Isothermal crystallization energy from experiments at 320 K vs. time for samples A, B, C, D, and E.

ference in Δh_{cc} between sample A and E is retained to 15 J/g throughout the whole cooling rate interval. In Figure 6, we show the isothermal crystallization energy (Δh_{ci}) as a function of time at 320 K. The general trend agrees with the continuous cooling crystallization results, showing that samples with lower mean molecular weight, crystallizes faster and to a higher extent. Our samples have half crystallization times ($t_{1/2}$), varying from 700 to 3600 s. As in the continuous cooling case, sample C deviates from the trend by showing the fastest crystallization of all samples, which we interpret as being due to heterogenities giving better nucleating properties. As in the case of continuous crystallization, adding 2% of polyethylene to sample A markedly increased the crystallization rate. The half crystallization time at 320 K decreased from 1000 to about 460 s. In this temperature range, the overall crystallization is strongly dependent on the nucleation conditions. In Table II we show the $t_{1/2}$ values of the unseeded samples at 316 and 320 K. The results of the isothermal crystallization process at 320 K and the continuous crystallization that occur at the lower cooling rates yield approximately the same heat of crystallization. Both the isothermal and the continuous cooling crystallization gives slightly lower crystallization degree than the results on melting. The difference is small for sample A, less than 2 J/g, but increases to 7 J/g for sample E. This means that no decisive crystal perfection or other molecular

Table II Mean Values and Standard Deviation of the Avrami and Ozawa Exponents Deduced from Fits of Eqs. (2) and (6), Respectively

	Avrami		Ozawa		$t_{1/2}$ graph/s		$t_{1/2}$ eq. 4/s	
Sample	n	σ	n	σ	T = 316 K	T = 320 K	T = 316 K	T = 320 K
A	3.1	0.10	2.9	0.14	260	1000	200	900
B	3.2	0.15	3.6	0.17	350	1660	350	1680
C	3.3	0.10	3.6	0.06	190	690	190	660
D	3.6	0.15	3.5	0.14	440	2260	440	2260
E	3.5	0.10	3.4	0.12	680	3600	690	3580

The number of measurements that the given values are based on can be deduced from figure 7, i.e two for the Avrami and 3–6 for the Ozawa analyses. Last columns show the half crystallization time in seconds, determined graphically and from equation 4.

rearrangement occur during reheating for the lower molecular samples, but that this is the case for the other samples.

Avrami Analysis

In the further analysis of the isothermal results, we have used the ordinary Avrami equation to characterize the overall kinetics of crystallization.

$$1 - X(t) = \exp(-kt^n) \quad (1)$$

Here, $X(t)$ is the crystalline fraction, t is the time, k is the overall crystallization rate constant that is a combined function dependent on both nucleation and growth rates. The Avrami exponent (n), depends both on the nature of the nucleation and on the growth geometry.[25] The equation above can be linearized as

$$\ln\{-\ln[1 - X(t)]\} = \ln(k) + n\ln(t) \quad (2)$$

The theory predicts that, for three dimensional spherulitic growth, an Avrami exponent of $n = 3$ corresponds to athermal, meaning simultaneously formed nucleus, while a value of 4 indicates thermally or sporadic nucleation. The Avrami theory was initially derived for small molecules, and there are some limitations regarding the application to macromolecules. Some of the problems are briefly mentioned below, whereas an extensive discussion is done by Wunderlich.[25] Equation (1) is based on a two-state model where the densities of these crystalline and liquid regions are approximated to be constant in time. Further, the radial growth rates of the spherulites are assumed to be constant and the nucleation mode unique. As the crystallization proceed and neighboring crystallites begin to impinge, the crystallization will deviate from the Avrami expression and show a slower growth rate. However, at crystallinities below this limit, experimental data show a linear behavior according to eq. (2). Hay and Przekop[26] have done calculations of the effect on the Avrami parameters n and k for some of the limitations of the Avrami theory when applied to polymers. They concluded that the Avrami equation is a reasonable approximation to most systems, except when a change in radial density occurs. Grenier and Prud'homme[27] point out the importance of careful determination of the experimental parameters, $X(t)$ and t, to avoid errors in the Avrami parameters. The fit of the Avrami equation to the isothermal data at 316 and 320 K gives n values about 3 for sample A, while the other samples in general have values closer to 3.5. No temperature dependency of the exponents was found, and in Table II, we show the mean n values with standard deviation from both Avrami and Ozawa analysis. The deviation from the Avrami equation as discussed above sets in as early as at a crystallinity close to 45% for sample A, where the other samples follow the Avrami expression up to crystallinities of 60–80%. The results indicate that all samples crystallize in a spherulitic morphology, and that athermal nucleation dominates. Samples cooled from the melt at a rate of 1 K/min to room temperature and studied in a microscope under crossed polarizers show a maltese crosspattern, characteristic for spherulitic morphology. The radius of the impinged spherulites are about 25–50 μm for the samples. Considering the Avrami exponent of PCL, we find that literature data collected by Wunderlich[25] give n values of 3 for samples of molecular weights (M_w) between 700 and 22,000 at temperatures between 318 K and 327 K. Goulet and Prud'homme[28] give values between 2.5 and 3.5 for temperatures ranging from 313 to 322 K and M_w = 48,000, whereas a value of 3 for temperatures 308–321 K and M_w = 17,600 is reported by de Juana and Cortazar.[22] Chynoweth and Stachurski[29] show data that are close to 4 for a sample of mean molecular weight of 85,000 and at a temperature of 319.5 K. They also reported linear growth rates but observed a change in nucleation rate during the early stages of the crystallization. From optically observed nucleation rate data, they found that a fit of the Avrami equation only gave integer values of the exponent. Phillips et al.[30] found, for low molecular species (M_w = 7000) and in the early stages of crystallization, a change in growth rate coupled to the change in morphology, from nonspherulitic to spherulitic. For the higher mean molecular species (M_w = 40,000), no change was observed.

When primary nucleation rates and growth rates for polymers have been detemined separately, both these properties have been found to have a negative temperature dependency at temperatures close to the melting point. This observed nucleation behavior is expected from the decreasing supercooling and coupled to the decreasing driving force for primary nucleation. The temperature dependency of the growth rate has been explained in a model consisting of surface or secondary nucleation followed by segmental transport over the liquid/crystal interface.[31] Thus, at small supercooling, the surface nucleation limits the growth rate. The rate constant, k in the Avrami equation, is a combined function of nucleation and growth rates. In the case of simultaneously nucleation, it has the same general temperature dependency as the growth rate, and can be written as

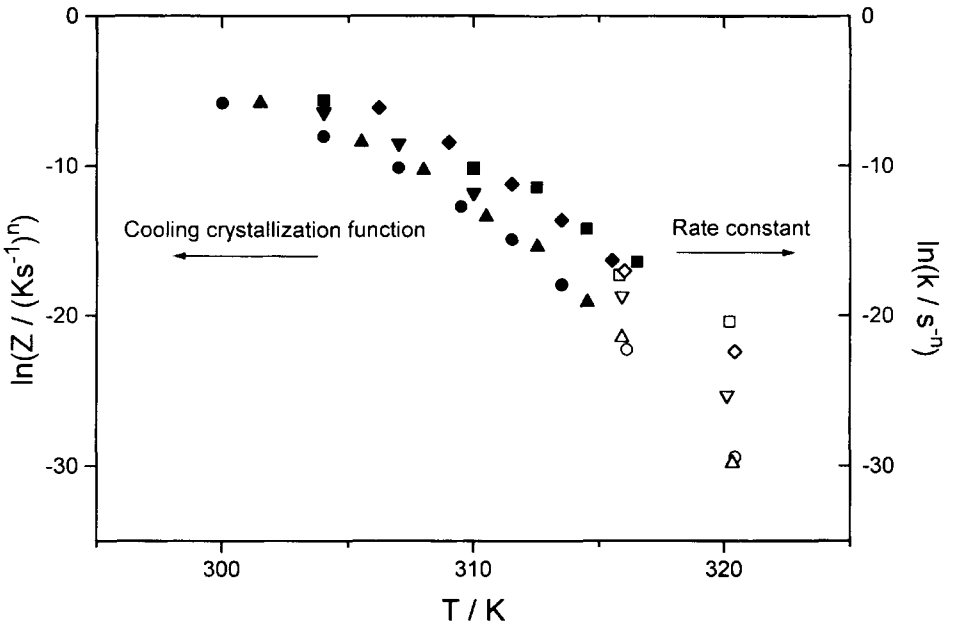

Figure 7 Rate constants from fits of eq. (2) (open symbols; scale at the right) and cooling crystallization functions from fits of eq. (6) (closed symbols; scale at the left) vs. temperature. Labels: Squares sample A, down triangle sample B, diamond sample C, up triangle sample D, circles sample E.

a product of two exponentials. These are influenced by mobility and surface nucleation, and equations like (3) below are often used to describe the temperature dependence of these two processes.[22,31,32]

$$k = k_0 \exp\left(\frac{-A}{R(T_c - T_\infty)}\right)\exp\left(\frac{-BT_m}{T_c \Delta T}\right) \quad (3)$$

A here is proportional to the activation energy for chain mobility, T_c the crystallization temperature, T_∞ a temperature below the glass transition where the chain mobility ceases, and R finally the gas constant. In the nucleation exponential, ΔT is the supercooling and T_m is the melting temperature. B reflects surface energy of the nucleus, lattice energy of the crystal, and the rate of which new nucleus are connected to the crystal surface. The nucleation limits the crystallization rate at small supercoolings, while the molecular mobility becomes the dominating feature at higher supercoolings. At temperatures approximately halfway between the melting point and the glass transition, eq. (3) above give a maximum where the two terms are of the same magnitude. In Figure 7 we show the temperature dependency of the rate constant and the continuous cooling crystallization function, $\ln(Z)$ from the Ozawa theory discussed below. We find that $\ln(k)$ increases with decreasing temperature, which is typically for a nucleation controlled process. The rate constants decrease in general with molecular weight. At 316 K, the low molecular samples have a rate constant about 200 times larger than the high molecular samples; this difference increases to 8000 at 320 K.

The half crystallization time, $t_{1/2}$, has properties related to the rate constant and is often used as a measure of the overall crystallization rate. If the crystallization follows the Avrami expression, the half-time values can be deduced from eq. (1) as:

$$t_{1/2} = \left(\frac{\ln 2}{k}\right)^{1/n} \quad (4)$$

In Table II we compare the half-time values calculated with eq. (4) with those obtained graphically from the experimental data and, thus, independent of any particular crystallization model. We find a good agreement for all samples, except for sample A, which showed a deviation from the Avrami expression at a relatively low conversion degree of about 45%. As in the case of the rate constant, the half-time values may be understood as a function of two competing processes, nucleation and molecular mobility. At high temperatures, that is, at low supercooling, the nucleation rate is the determining

process while, at lower temperatures, the molecular mobility becomes dominant. The $t_{1/2}$-value increases with temperature and fortifies that the crystallization process is controlled by nucleation in this temperature interval. As can be seen, the $t_{1/2}$-values increases in general with molecular weight. Sample C deviates from this trend by showing the lowest half crystallization times of all samples. In accordance with the high crystallization temperature of sample C (Fig. 3), we interpret the low $t_{1/2}$-value as a result due to heterogenities.

Ozawa Analysis

Only a few methods to analyze nonisothermal crystallization kinetics have been developed.[33-35] In this article, we use the method by Ozawa,[33] who extended the Avrami equation to constant cooling conditions. One advantage of his method is, thus, the possibility to compare the continuous cooling results with the isothermal results extracted by the Avrami equation. The model requires that crystallization occurs at constant cooling rate and that the nuclei grow as sperhulites. From these assumptions, Ozawa deduced the following expression for the untransformed material fraction.

$$1 - X(T) = \exp[-Z(T)(1/\dot{T})^n] \quad (5)$$

or

$$\ln\{-\ln[1 - X(T)]\} = \ln[Z(T)] + n \ln(1/\dot{T}) \quad (6)$$

Here, $X(T)$ is the crystalline fraction, $Z(T)$ is the cooling crystallization function, which is a complicated function of nucleation and growth rates. $\dot{T}$ is the absolute value of the cooling rate and n is the Ozawa exponent. In the Ozawa equation, neither the secondary crystallization nor the fold length of the polymer chain are considered. However, as reported by Ozawa[33] and Lopez and Wilkes,[36] the secondary crystallization will be very small due to the continually decreasing temperature. A linear fit of the left hand of eq. (6) vs. the logarithm of the inverse cooling rate at a given temperature gives the Ozawa exponent and the cooling crystallization function. Due to the rather fast crystallization and a restricted number of possible cooling rates with the calorimeter, we are limited to three consecutive cooling rates at each temperature. Further, due to the different crystallization degrees and crystallization rates, the number of reliable fits of the samples differ. This explains the different numbers of $\ln[Z(T)]$-values given in Figure 7. A representative result of a plot according to eq. (6) for sample A is shown in Figure 8. One benefit with the Ozawa approach is its possibility to analyze the crystallization kinetics at temperatures lower than the traditional isothermal Avrami method. However, in the investigated temperature interval from 320 down to 300 K, none of the samples show any conclusive temperature dependence in the exponent. We find an Ozawa exponent near 3 for sample A, while the other samples have exponents about 3.5. In Table II, we present the mean values and the standard deviation of the Ozawa and Avrami exponents. The agreement between the isothermal and nonisothermal results are acceptable.

The cooling crystallization function, $\ln[Z(T)]$, shows a similar temperature dependency as the isothermal rate constant $\ln(k)$ (see Fig. 7). This supports the argument that the cooling crystallization function is related to the overall rate of crystallization.[36,37] As in the case of the rate constant for isothermal crystallization, the $\ln[Z(T)]$-values increases with decreasing temperature for all samples. This indicates that nucleation is still the dominating feature at this lower temperature region where the $\ln[Z(T)]$-values are evaluated. A decrease in the cooling crystallization function with temperature has also been reported for PET,[33] PPS,[36] some n-paraffins,[37] and iPP.[38] However, at the lowest temperatures, close to 300 K, a decrease in the slope is clear, pointing to an increasingly influence of the competing mechanism of mass transport. The temperature where the maximum growth rate occurs can be estimated by the empirical relation $T = \theta(T_m - T_\infty) + T_\infty$ derived by Gandica and Magill and found in the compilation by van Krevelen.[39] Here, $T_\infty = T_g - 50$, and T_m, T_g are the melting and glass transition temperatures, respectively, and θ is a constant about 0.64 for all "normal" polymers. Using 342 K as the melting temperature and 209 K as T_g, we get a maximum growth rate temperature close to 265 K. Li et al.[40] showed a calculated spherulitic growth rate curve vs. temperature giving a peak at about 285 K for a sample of M_w = 101,000 and polydispersity 2. Although the data points in Figure 7 are not characteristic enough to give a distinct curve shape, we find that a fit of the bell-shaped eq. (3) to our nonisothermal results points to peak values ranging from 260 to 290 K. Further, the similar behavior of the cooling crystallization function and the rate constant with changing molecular mass, increasing with decreasing molecular mass, also supports the argument that the Z and k parameters are

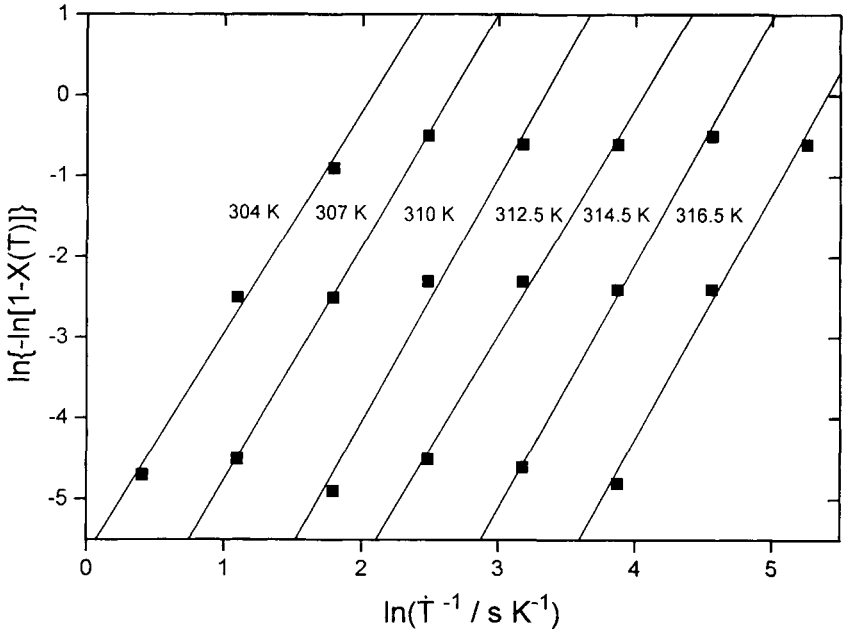

Figure 8 Double logarithm of the amorphous fraction vs. the logarithm of the inverse absolute cooling rate at different temperatures according to eq. (6) for sample A. The slopes of the lines corresponds to the Ozawa exponent at the indicated temperatures, while the cooling crystallization functions is deduced from the intersection of the lines with the ordinate.

related. At temperatures close to 315 K, the value of the cooling crystallization function is about 200 times larger for the low molecular weight samples than for the high molecular samples, thus showing the substantial kinetic differences between the samples.

CONCLUSIONS

The kinetic differences, as shown by half crystallization values, the rate constant, and the cooling crystallization function of the samples are very substantial in the investigated molecular weight and temperature range. As expected, samples of higher molecular weight show slower kinetics. Close to 315 K, both the Avrami rate constant and the Ozawa cooling crystallization function are about 200 times lower for the high molecular samples, while the half crystallization time increases with a factor of about 4. As a consequence, these samples will crystallize to a lower degree and this will take a longer time. However, in this regime 300 to 320 K where nucleation is the rate limiting process, the effect of seeding will reduce the influence from increasing molecular weight. At the lowest temperatures, the cooling crystallization function shows a decreasing slope, interpreted as an increasing chain mobility dependency on the crystallization. None of the samples show any conclusive temperature dependency in the Avrami and Ozawa exponents. The sample of lowest molecular weight has an exponent close to 3 from both Avrami and Ozawa analyses. The other samples have values closer to 3.5. All together, the results from the Avrami and Ozawa models together with the observations in the optical microscope suggest that all samples crystallize in a spherulitic morphology independent of the investigated crystallization procedures.

The authors are grateful to Dr. P. van de Witte at the University of Twente, Enschede, Netherlands, for supplying some of the PCL samples. This work was financially supported by the Swedish National Board for Industrial and Technical Development (NUTEK).

REFERENCES

1. C. G. Pitt, *Drugs Pharmaceupt. Sci.*, 71 (1990).
2. C. G. Pitt, F. I. Chasalow, Y. M. Hibionada, D. M. Klimas, and A. Schindler, J. *Appl. Polym. Sci.*, **26,** 3779 (1981).

3. M. Yasin and B. J. Tighe, *Biomaterials,* **13,** 9 (1992).
4. J. Kaloustian, A. M. Pauli, and J. Pastor, *J. Therm. Anal.,* **37,** 1767 (1991).
5. S. Akahori and Z. Osawa, *Polym. Degrad. Stabil.,* **45,** 261 (1994).
6. F. Lefebvre, C. David, and C. Vander Wauven, *Polym. Degrad. Stabil.,* **45,** 347 (1994).
7. Y. Yakabe and H. Tadokoro, *Chemosphere,* **27,** 2169 (1993).
8. M. Kamimoto, Y. Abe, S. Sawata, T. Tani, and T. Ozawa, *J. Solar Energy Eng.,* **108,** 282 (1986).
9. M. Kamimoto, Y. Abe, K. Kanari, Y. Takahashi, T. Tani, and T. Ozawa, *J. Solar Energy Eng.,* **108,** 290 (1986).
10. Y. Abe, Y. Takahashi, R. Sakamoto, K. Kanari, M. Kamimoto, and T. Ozawa, *ASME J. Solar Energy Eng.,* **106,** 465 (1984).
11. K. V. Liu, U. S. Choi, and K. E. Kasza, *Measurements of Pressure Drop and Heat Transfer in Turbulent Pipe Flows of Particulate Slurries,* ANL-88–15, Argonne National Laboratory, Argonne, USA, 1988.
12. K. E. Kasza, S. U. Choi, and J. Kaminsky, *Ashrae Transact.,* **93,** 2 (1987).
13. K. E. Kasza and M. M. Chen, *J. Solar Energy Eng.,* **107,** 229 (1985).
14. K. Hayakawa, H. Taoda, M. Tazawa, and H. Yamakita, Proc. 1989 Congress Int. Solar Energy Society, Kobe, Japan, vol. 3, 2281 (1990).
15. T. L. Vigo and J. S. Bruno, Proc. 26th Intersociety Energy Conversion Eng. Conference, Boston, MA, vol. 4, 161 (1991).
16. P. Skoglund and Å. Fransson, *Thermochim. Acta,* **277,** 27 (1996).
17. M. J. Richardson, *Comprehensive Polymer Science, Vol. 1, Polymer Characterization,* G. Allen, Ed., Pergamon Press, New York, 1989, p. 867.
18. M. Alsleben, C. Schick, and W. Mischok, *Thermochim. Acta,* **187,** 261 (1991).
19. M. Alsleben and C. Schick, *Thermochim. Acta,* **238,** 203 (1994).
20. B. Lebedev and A. Yevstropov, *Makromol. Chem.,* **185,** 1235 (1984).
21. Advanced THermal AnalysiS (ATHAS), Databank of thermodynamic properties of linear macromolecules and small molecules. Copyright Prof. B. Wunderlich, Department of Chemistry, University of Tennessee, Knoxville, TN.
22. R. de Juana and M. Corta'zar, *Macromolecules,* **26,** 1170 (1993).
23. V. Crescenzi, G. Manzini, G. Calzolari, and C. Borri, *Eur. Pol. J.,* **8,** 449 (1972).
24. H. Ishida and P. Bussi, *J. Mater. Sci.,* **26,** 6373 (1991).
25. B. Wunderlich, *Macromolecular Physics,* Vol. 2, Academic Press, New York, 1976, p. 132.
26. J. N. Hay and Z. J. Przekop, *J. Polym. Sci.,* **17,** 951 (1979).
27. D. Grenier and R. E. Prud'homme, *J. Polym. Sci.,* **18,** 1655 (1980).
28. L. Goulet and R. E. Prud'homme, *J. Polym. Sci.,* **28,** 2329 (1990).
29. K. R. Chynoweth and Z. H. Stachurski, *Polymer,* **27,** 1912 (1986).
30. P. J. Phillips, G. J. Rensch, and K. D. Taylor, *J. Polym. Sci.,* **25,** 1725 (1987).
31. J. H. Magill, *Treatise on Materials Science and Technology, Vol. 10, Properties of Solid Polymeric Materials,* Part A, J. M. Schultz, Ed., Academic Press, Inc., New York, 1977, p. 247.
32. M. Day, Y. Deslands, J. Roovers, and T. Suprunchuk, *Polymer,* **32,** 1258 (1991).
33. T. Ozawa, *Polymer,* **12,** 150 (1971).
34. A. Ziabecki, *Appl. Polym. Symp.,* **6,** 1 (1967).
35. K. Nakamura, K. Katayama, and T. Omano, *J. Appl. Polym. Sci.,* **23,** 1031 (1973).
36. L. C. Lopez and G. L. Wilkes, *Polymer,* **30,** 882 (1989).
37. A. Hammami and A. K. Mehrotra, *Thermochim. Acta,* **211,** 137 (1992).
38. G. B. A. Lim and D. R. Lloyd, *Polym. Eng. Sci.,* **33,** 529 (1993).
39. D. W. Van Krevelen, *Properties of Polymers,* 3rd ed., Elsevier Science Publishers B.V., Amsterdam, 1990, p. 585.
40. W. Li, R. Yan, X. Jing, and B. Jiang, *J. Macromol. Sci.,* **B31**(2), 227 (1992).

Received January 23, 1996
Accepted April 2, 1996